Draft Release

Global Tools to Unlock Capital for Investments in Nature-Based Solutions

METHODS REPORT

GLOBAL CENTER ON ADAPTATION

Environmental Change Institute 2025

AUTHORS & ACKNOWLEDGEMENTS

This report was developed by

Environmental Change Institute, University of Oxford

Tom Harwood, Tom Russell, Carlo Pasqua, Minerva Singh, Tim Fowler, Jim Hall

Global Center on Adaptation:

María José Vásquez, Martin Garcia Perez, Edwina Mercer, Sertac Turhal, Adele Cadario

DESCRIPTORS

Global, Nature Based Solutions, Mangroves, Landslides, Flooding, Infrastructure, Investment

Acknowledgements:

GLOBAL CENTER ON ADAPTATION

ABOUT THE GLOBAL CENTER ON ADAPTATION

The Global Center on Adaptation (GCA) is an international organization, hosted by the Netherlands, which works as a solutions broker to accelerate action and support for adaptation solutions from the international to the local, in partnership with the public and private sector, to ensure we learn from each other and work together for a climate resilient future.

In Partnership with:

eci UNIVERSITY OF OXFORD

ABOUT THE ENVIRONMENTAL CHANGE INSTITUTE

The Environmental Change Institute at the University of Oxford was formed in 1991 as an interdisciplinary research institute focusing on the complex processes of global environmental change, the exploration of sustainable solutions and motivating change for the better through partnerships and education.

1. CONTENTS

2. ABBREVIATIONS

Acronyms	Definitions
AAL	Average Annual Loss
BHI	Biodiversity Habitat Index
DEM	Digital Elevation Model
EAD	Expected Annual Damages
GCM	Global Circulation Model
NbS	Nature Based Solutions
ROI	Return on Investment
RCP	Representative Concentration Pathway
RP	Return Period
USD	United States Dollars

3. EXECUTIVE SUMMARY

This document is the methods report for the Global Tools to Unlock Capital for Investments in Nature-Based Solutions Project. This work developed a fine-resolution global tool to highlight areas where nature-based solutions (NbS) in the form of viable tree planting have the potential to reduce risk to infrastructure, through flood reduction, coastal erosion control and landslide risk reduction.

The outputs are a series of maps showing potential opportunity areas for revegetation with trees at a 250m resolution globally, with their associated costs, and potential biodiversity and carbon co-benefits, and tools to allow exploration of these areas in terms of their potential avoided damages and return on investment. As a global scale assessment, making use of globally consistent and publicly available datasets, there are likely to be limitations on the accuracy of the information provided at the fine spatial scale, and these results are targeted at the initial project screening stage, to select between broad areas and understand the regional context. After this initial screening, users should follow up with more detailed studies, drawing on best available local information to develop an in depth understanding of the potential costs and benefits of an individual project.

The work covers three categories of risk reduction:

- Mangrove restoration for reduction of coastal erosion. This is divided into 3 categories, areas with accreting shorelines, areas with neutral to slowly retreating shorelines and areas with fat retreating shorelines, with respective increasing costs in relation to coastal management;
- Tree restoration for the reduction of landslide risk. These are divided into two categories, areas which replace crops (since in some cases the landslide risk may be exacerbated by agricultural activities, and this costly option might be appropriate) and other areas. An additional category where the ground is currently bare is also highlighted. This is a rare case, and may indicate that there is insufficient soil for tree growth;
- Sub basin level plantings for potential flood risk reduction. Here sub basins with risk of flooding are identified, and all potential tree plantings in the sub basin flagged. A variety of different planting approaches can be used to manage flooding, but all require a significant extent of plantings to make a difference. Due to the complexity of river flow, and limited evidence, no downstream effects outside the immediate catchment are considered.

For each category, two types of restoration are considered, natural regeneration or assisted native plantings. Carbon potential is assessed as a final density of carbon for mature restoration. Whilst for mangrove ecosystems the additional below ground carbon effect of mangrove biomass in estuarine mud and beaches is considered, soil carbon in terrestrial system is not considered due to conflicting context-specific effects of tree planting on soil carbon, which are not fully understood.

Risks of direct damage are calculated for road and rail infrastructure, using return period hazard maps (flooding) or probability of occurrence (landslide) with damage curves and reconstruction/rehabilitation costs to estimate expected annual damages (EAD) in the current situation, before any NbS intervention. Opportunity areas are identified as patches suitable for planting within each sub-basin, attributed with total area, planting costs, biodiversity and carbon benefits, and the current level of risk to infrastructure posed by each hazard.

The input data and results are visualised within the GRI Risk Viewer, publicly available online, to allow exploration of risks and hazards to infrastructure and potential avoided damages. An Excel tool is also developed, aiming to support financial decision-making. This takes the opportunity areas and calculates additional metrics to support prioritisation and screening of potential investments

4. INTRODUCTION

4.1 Overview

Nature based solutions are a class of management action where natural systems are supported or restored in order to bring benefits to humans and to nature. A typical example is the planting of trees for climate change mitigation. Rather than planting a monoculture, more natural plantings can support native biodiversity, provide recreational benefits to humans and in some cases sequester more carbon in a more sustainable manner. In this work, we examine nature-based solutions in the form of native tree restoration to protect infrastructure, in both terrestrial woodland and mangrove ecosystems. Three classes of risk, coastal erosion, landsliding and flood risk are examined. Estimated restoration costs, and carbon and biodiversity co-benefits are estimated for each pixel. The analysis was conducted at a 9 arc second (approximately 250m*250m) grid cell size. It should be noted that there are limitations to the accuracy of data at this scale and resolution, both in the inputs, and flowing through to the outputs, so whilst the information is suitable for initial project screening, any investment decisions should be made after more rigorous spatial analysis using regionally accurate information. The basic analysis approach was to use the intersection of best available datasets. This report provides an overview of the final collated datasets and a detailed reproducible methodology.

Infrastructure systems provide essential services to economy and society. Physical infrastructure assets are at risk of damage due to multiple hydrometeorological and geophysical hazards. In this work, we assess riverine and coastal flooding and landslide risks to transport infrastructure (motorway, trunk, primary, secondary and tertiary roads and rail lines) and quantify the risk in terms of expected annual damage (EAD) at the asset level (road or rail link). The risks to infrastructure are then linked to potential opportunity areas for nature-based solutions, along with the restoration costs and carbon and biodiversity co-benefits. This analysis is carried out using the OpenGIRA (Open Global Infrastructure Risk/Resilience Analysis) workflow, which is available as open-source code to support reproducibility and extensibility. This report details the infrastructure and hazard datasets used for risk analysis and the methodology which produces the dataset of opportunity areas.

The GRI Risk Viewer online tool presents the opportunities and hazards on an interactive map for exploration and prioritisation at national and sub-national scales. These data are also imported to a Microsoft Excel based tool which facilitates investment decision making. This report describes the methods implemented in the Excel tool. Separate user guides provide further details of each tool.

5. METHODS 1: OPPORTUNITY AREAS

5.1 Overview

Due to differences in both ecology and data, different approaches were taken to assess the opportunity areas and benefits for the terrestrial and coastal mangrove systems for each of the stages of spatial analysis.

5.2 Base map

The 9s base map used for the analysis was the 250m WGS84 resampled MERIT Digital Elevation Model dataset from Hengl (2018). All other data was resampled to align with this grid prior to data processing. Upscaling was conducted by cell aggregation followed by bilinear resampling. Downscaling was conducted by bilinear resampling. Where necessary data was gap filled using Euclidean Distance Allocation followed by Low Pass Filtering. For large areas with missing data, (such as planting costings in high latitudes), either global means or percentile values as appropriate were used. Since mangrove systems necessarily extend beyond the shoreline, the MERIT DEM land mask was extended to account for potential restoration sites.

5.3 Potential tree restoration areas

5.3.1 Terrestrial systems

Viable areas for new tree plantings or restoration were defined as areas with

- The potential for tree growth
- Minimal existing tree cover
- No conflicting land use (built up areas and crops)

Potential for tree growth was calculated by first aggregating all tree biome classes from the Hengl et al. (2018) dataset at 30s (1km) resolution, and masking all cells with a sum probability of tree growth less than 0.75. An additional filter was applied since many landslides occur in high altitudes, to remove all areas above the treeline. The TREELIM model (Paulsen and Körner, 2014) was calculated from the CHELSA climate dataset (Brun et al., 2022) at 1km resolution. After intersecting these two surfaces, the resultant map was resampled using bilinear interpolation to 250m and only cells with a greater than 0.5 probability retained.

The Copernicus Global Land Cover layers for 2020 (Buchhorn et al., 2020) were used as the source of all landcover information in this study. Rather than use the discrete product, (which would be difficult to upscale) the probability surfaces for each land cover class (Trees, Built-Up, Crops, Bare) were aggregated and resampled from 100m to the base map 250m resolution. For each class, all cells with >0.25 probability of a that class were converted to a binary mask, which was used in all subsequent analyses.

The potential vegetation mask was then intersected with the landcover layers, and built-up and already tree covered areas were excluded. Cropped areas were excluded for flood reduction, and for the baseline landslide areas. However, since in some cases, landslide risk is exacerbated by agriculture on inappropriate slopes, these areas suitable for landslide risk reduction, but currently cropped were separately mapped. The workflow is illustrated in Figure 1 below.

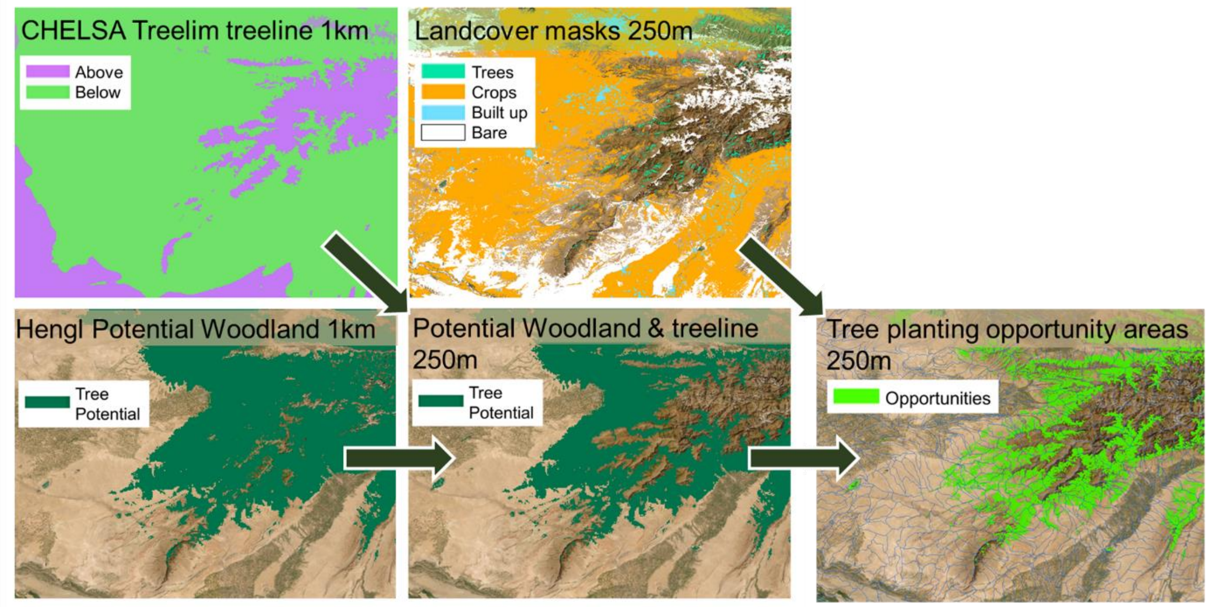

Figure 1 : Workflow for the identification of terrestrial tree planting opportunity areas.

5.3.1.1 Landslide risk reduction opportunities

Areas with the potential for tree planting and restoration to reduce landslide risk were identified as a subset of the potential tree opportunity sites. All areas with non-zero landslide hazard as identified in the World Bank Global Landslide Hazard Map (Redshaw, 2020, The_World_Bank_Group, 2021) following resampling from 1km to 250m. A slope mask was used to identify areas with potential to reduce landslide risk, based on (Kasai and Yamada, 2019, Lan et al., 2020, Li and Duan, 2024). MERIT DEM derived slope at 250m was used, noting that there could be considerable within variation in slope at this scale, so a conservative range was used. Planting on slopes below 8° was assumed to have no remedial effect. Indeed, landslide hazard below 10° is negligible, but some increased stability and physical barrier protection might be expected. The upper limit is more significant, since planting on steeper slopes above 45° is likely to decrease stability. In this case, only areas below 36° were considered suitable. The resultant layer was intersected with the tree opportunity areas. Areas which would replace crops were flagged as mentioned above for further investigation, as well as bare ground areas which might be unsuitable for other reasons.

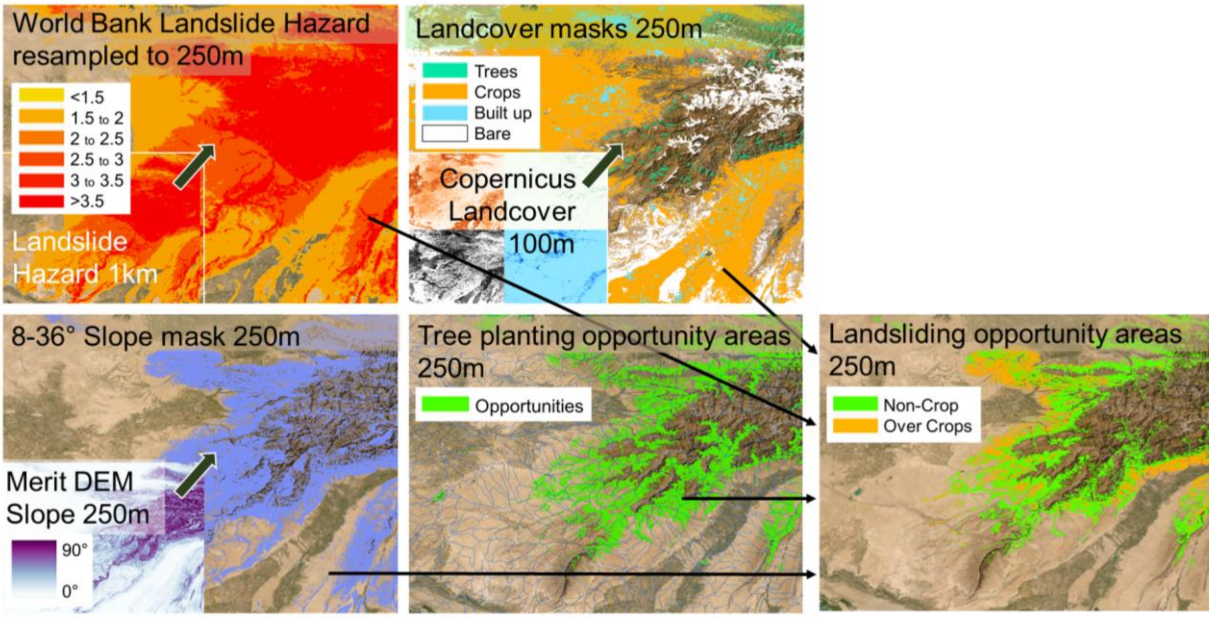

Figure 2 : Workflow to identify potential landslide hazard risk reduction

A 3km radial buffer for potential risk reduction for landslides was selected, based on a medium to large landslide size from (McColl and Cook, 2024)

5.3.1.2 Riverine flood risk reduction opportunities

A method summary is presented here for consistency, but the full method is described in Chapter 7. Flood risk was derived from a range of different flood products, but a simple consistent approach was used to filter the tree Opportunity areas. Firstly a coastal (Sayre et al., 2019) buffer of 3km was excluded from the tree opportunities map, since trees are unlikely to have any riverine flood risk impact close to river outlets, and to exclude the majority of coastal flooding. Flood risk and opportunities were aggregated by the smallest (level 12) basin classification of the HydroBasins global polygon data (Lehner, 2013). A threshold for expected annual damages from flooding to infrastructure was applied and only sub basins above this threshold containing tree NbS opportunities were selected. A simplified visual representation is shown in Figure 3 below.

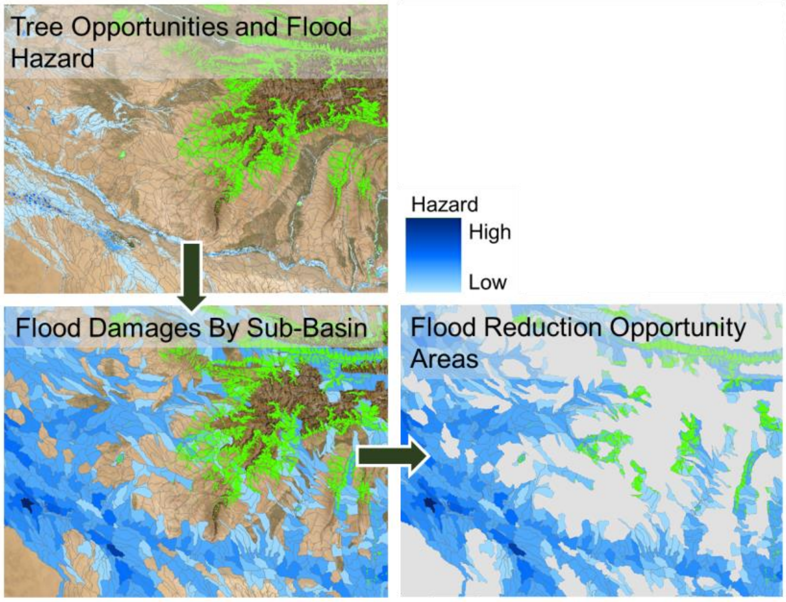

Figure 3 Simplified workflow for identification of riverine flood risk reduction opportunities.

5.3.2 Mangrove systems

Viable areas for new plantings or restoration were defined as areas

- Within 10km of existing mangroves
- Falling between high and low tides
- Within 1km of the current coastline

This approach drew heavily on the open access data mangrove opportunity screening and opportunity classification approach of Gijón Mancheño et al. (2021), with the addition of more nuanced tidal ranges, and a coastline distance limitation to facilitate reliability at the global scale (i.e. to avoid inland areas being accidentally selected).

The first step was the development of the intertidal elevation data. Examination of the MERIT DEM (Hengl et al., 2018) and FABDEM (Hawker and Neal, 2021) showed poor land surface discrimination in mangrove regions, but the third version of CoastalDEM (Kulp and Strauss, 2024) at 90m resolution proved to treat this difficult problem reliably. A representation of the intertidal habitat one was achieved by merging the CoastalDEM v3 data with the GEBCO bathymetry dataset (GEBCO_Compilation_Group, 2023) following the workflow outlined below and shown in 4.

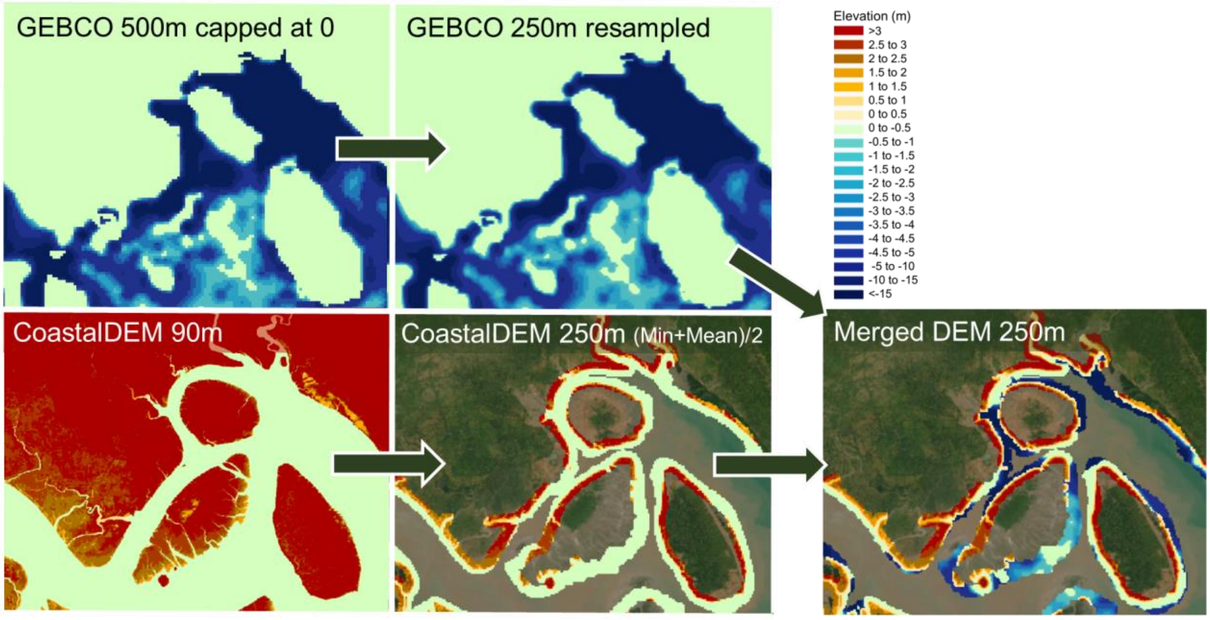

Figure 4 : Workflow for the calculation of intertidal elevation.

The GEBCO bathymetry data was first capped at 0m (since this is a synthesised DEM product which has not been coastally corrected for mangrove vegetation) and then resampled to 250m. The CoastalDEM data was aggregated to 250 by calculating both the mean and the minimum value of all 3s (≈90m) cells within each 9s (≈250m) cell and then calculating the average of these. Conceptually this approach was designed to capture cells with at least some suitable intertidal habitat. These two datasets were merged using resampled GEBCO below zero and resampled Coastal DEM at and above 0m. This dataset was further masked using a 1km buffer around the 30m resolution global shoreline vector of Sayre et al. (2019), which proved to be the most reliable shoreline dataset for small islands and estuarine mangrove systems. This 2km wide buffer may result in underestimation of potential habitat in some flatter coastal regions, but will also avoid overestimation, for example in freshwater lagoons and inland depressions.

The next step was to identify the mangroves opportunity areas (Figure 5). Initially this followed the Gijón Mancheño et al. (2021) approach, identifying all areas within 10km of existing mangrove areas in 2020 (Bunting, 2022) and creating a descriptor of shoreline change rates. The Shoreline Change Monitor dataset (Luijendijk et al., 2018) of 500m spaced transects was rasterised to 250m and then extended using Euclidean allocation to fill the coastal buffer. The subsequent layer was smoothed using a low pass filter prior to the original data points being superimposed. An additional component was then introduced to provide a better description of the intertidal zone, to draw on the information in the elevation/bathymetry layer. The Global Tidal Classification (van Graafeiland, 2020) derived from FES2014 (Lyard et al., 2021) was used to define simple definitions of intertidal. These are shown graphically in Figure 5, and were Microtidal (-0.5 to 0.75m), Mesotidal (-1.2 to 1.5m) and Macrotidal (-1.6 to 2m), with Undefined areas using a range of -1 to 1m. Potential opportunity areas falling within 10km of existing mangrove populations and within the intertidal range were classified into 3 categories using the shoreline change data. Consistent with Gijón Mancheño et al. (2021), the sites were split into those with accreting shorelines (which would need no coastal management) and those with retreating shorelines. For this latter class, a distinction was made between neutral to slow retreating and fast retreating (>5m over 20 years), on the basis that faster retreating sites would likely require more extensive (and expensive coastal management). These sites were left in to assist with planning larger restoration projects where some less ideal locations might need to be considered. Areas with existing conflicting land use in the form of crops or habitation (whilst unlikely in the intertidal zone) identified by the Copernicus land cover mapping (Buchhorn et al., 2020) and pixels with existing mangrove cover of >50% as calculated from either Bunting (2022) or Simard (2019) were excluded.

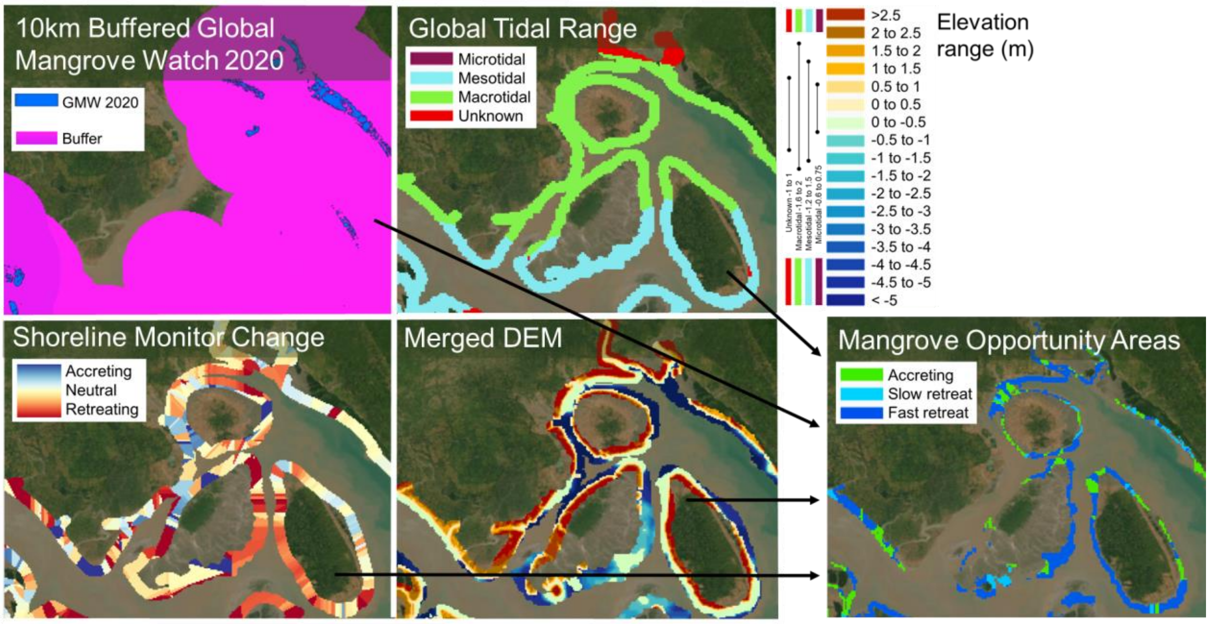

Figure 5: Workflow for the identification fo mangrove opportunity areas

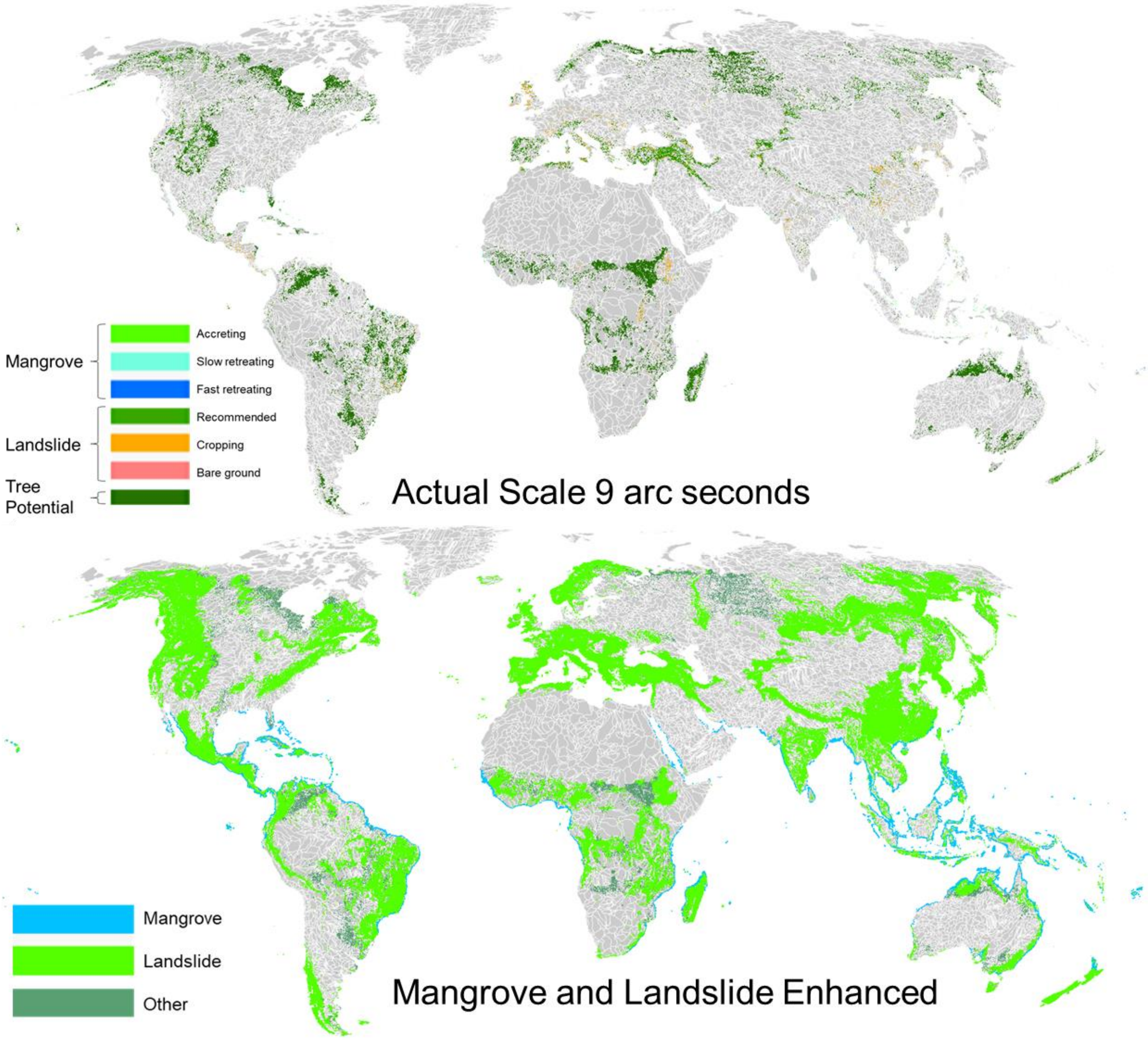

Figure 6 : Global map of opportunities, showing the results at the raw 9 arc second (250m) grid resolution (above) which shows how sparse these opportunities are, and below with mangrove and landslide reduction opportunities magnified to show broad opportunity regions.

6. METHODS 2: COSTS AND BENEFITS

6.1 Overview

Estimated planting costs were drawn mainly from Busch et al. (2024), supplemented by estimated coastal management costs for mangrove systems. Co-benefits in the form of carbon and biodiversity were also estimated. For biodiversity the marginal benefit of restoration per location was calculated from the global Biodiversity Habitat Index (Harwood, 2022, Hoskins et al., 2020), supplemented by an analysis of the Global Mangrove Watch (Bunting, 2022) dataset for mangrove systems. Carbon was calculated as the total additional carbon at maturity, which was used as the basis for simplified carbon accumulation curves assuming a 50 year growth period.

6.2 Revegetation and Planting Costs

6.2.1 Terrestrial systems

For terrestrial systems, the Busch et al. (2024) data was first extrapolated by 2km using euclidean allocation to fill variations in coastal definition and then resampled from 1km to the 250m grid (Figure 7Figure 1). For high and low latitudes, where there were no costings, all cells were set to the upper limit of the dataset excluding outliers at a constant value of $2000 per hectare for revegetation and $3500 per hectare for native plantings. In most of these areas of extrapolation, economic considerations are likely to be complex, and these constant figures should be considered loose estimates only. Similarly, the entire Busch et al. (2024), dataset will likely be subject to considerable local variation due to issues of site access and changes in economics over time. These figures do, however, provide a useful baseline estimate for further consideration of opportunities The final global maps for all land and mangrove areas can be seen in Figure 9. Costings were left as cost per hectare so that project costs could be estimated as a function of area, since not all project (especially linear opportunities) will take up a full grid cell.

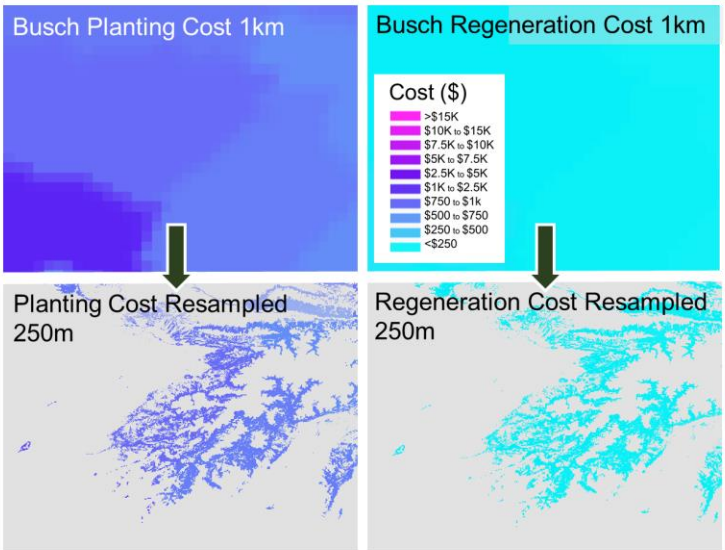

Figure 7 : Resampling of cost layers for terrestrial systems.

6.2.2 Mangrove systems

In mangrove systems the extrapolated Busch et al. (2024), costs described above were used as the baseline costing for accreting shorelines, where no additional management is required. For the slow and fast retreating shorelines., the approximate costs of minimal and extensive coastal management respectively were drawn from the literature (Bayraktarov et al., 2016, Hudson et al., 2015, The_World_Bank_Group, 2022). Resultant costs for both natural regeneration and native plantings were estimated as Cost*2*$2000 per hectare for slow retreating sites and Cost*3+$10000 per hectare for fast retreating sites. As can be seen this makes the fast-retreating sites (where extensive hard coastal management is required in addition to mangroves) expensive and likely cost-ineffective to restore, and are possible only worthwhile as a sub-component of a larger opportunity.

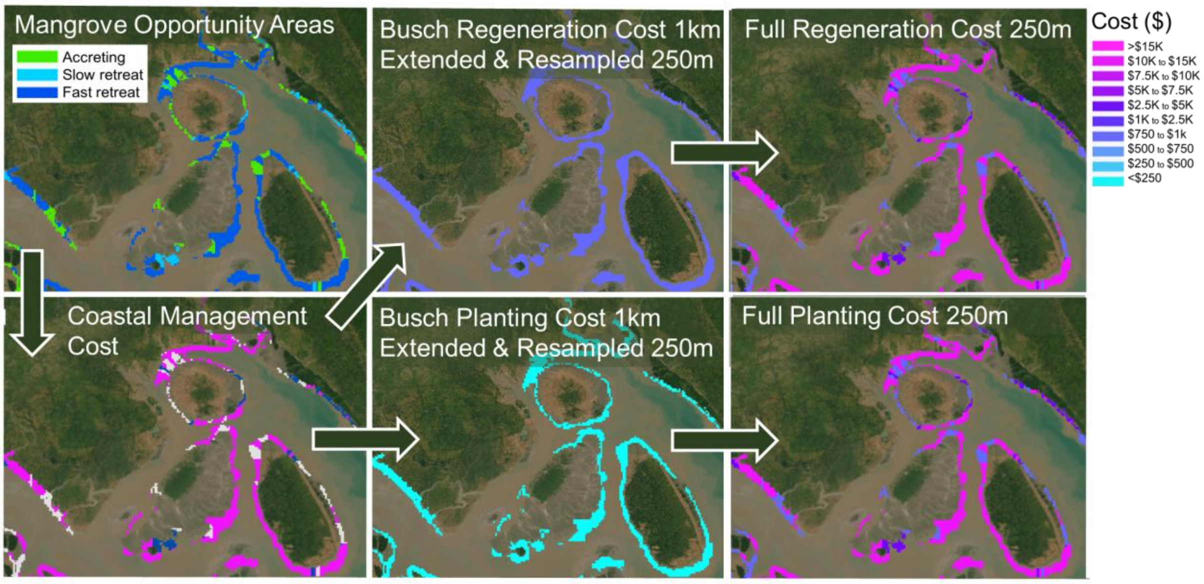

Figure 8 : Incorporation of coastal management costings for mangrove restoration

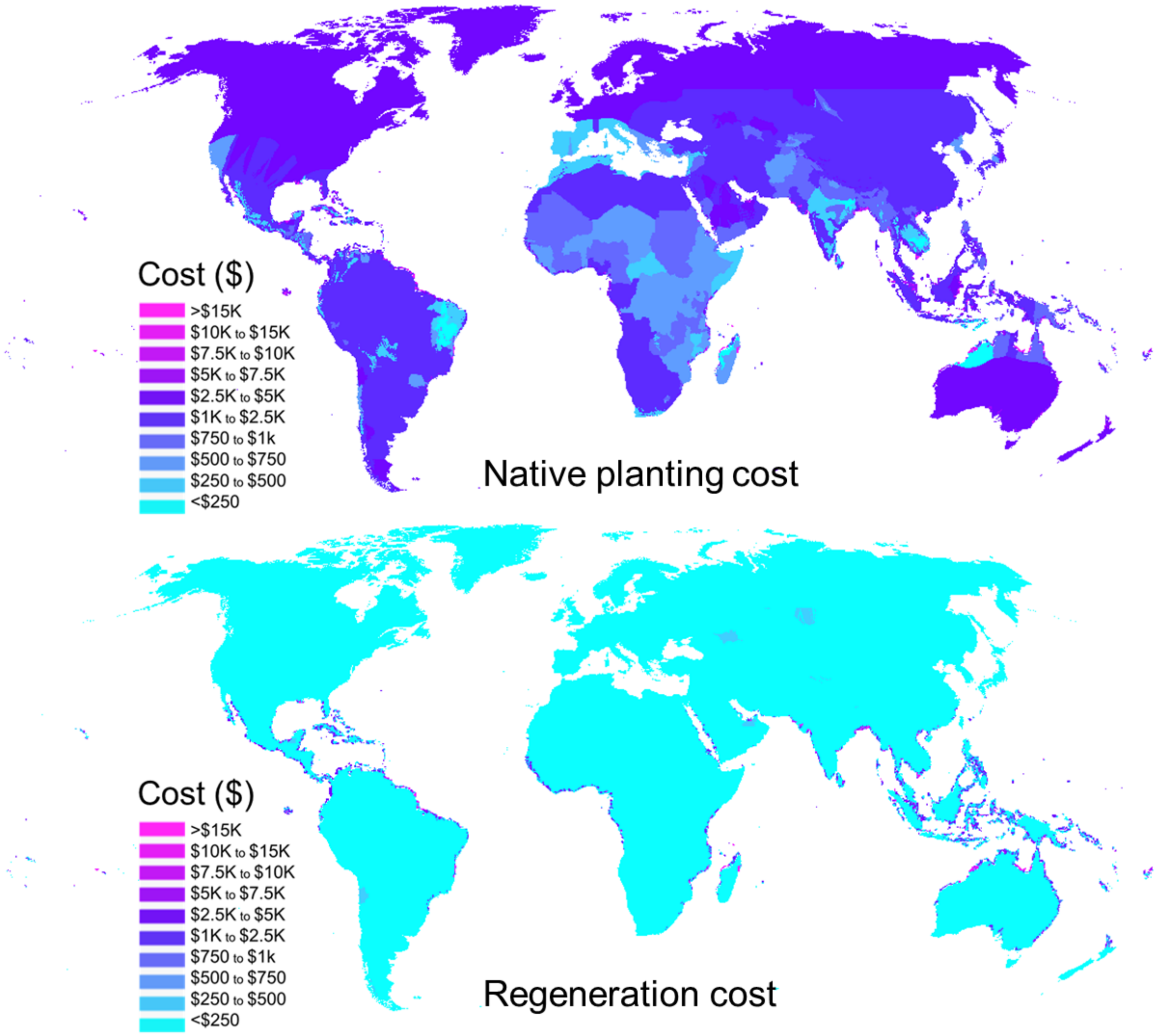

Figure 9 : Global opportunity costings, showing areas of extrapolation in high latitudes and Australia, and higher mangrove opportunity costs where coastal management is required.

6.3 Biodiversity Benefits

6.3.1 Terrestrial systems

For terrestrial systems the relative biodiversity benefit was taken as the marginal benefit of restoration of each grid cell, based on the global Biodiversity Habitat Index 2020 (Harwood, 2022, Hoskins et al., 2020), which is a Component Indicator for Goal A of the UN CBD Global Biodiversity Framework (UNCBD, 2022), showing the state of each 1km grid cell globally in 2020. Following the approach outlined in Allnutt et al. (2008), the relative marginal benefit of restoration actions in each grid cell was calculated as the first derivative (slope) of the species-area curve (taking an exponent of z= 0.25) for the species-level BHI as

$$Benefit = 0.25BHI_{sp}{}^{-0.75}$$

The resultant index (Figure 11) is higher areas where restoration will have more overall impact on biodiversity. This will tend to highlight areas with high degradation, where species are most at risk. The resultant layer was extrapolated 15km to cover all potential mangrove locations using Euclidean allocation and resampled to 250m.

6.3.2 Mangrove systems

The BHI is a terrestrial index and does not explicitly cover mangrove ecosystems. However, we may expect a broad correlation between the amount of coastal anthropogenic influence and that immediately inland. As stated above, the first estimate of mangrove biodiversity status was made by extrapolation of the BHI. To provide a more mangrove specific approach, however, the Global Mangrove Watch data was used to estimate the proportional loss of nearby mangrove systems (an equivalent measure to the BHI) by calculating the proportion of 2020 versus the 1996 extent from Bunting (2022). This proportion was calculated at 5, 10 and 50km radii for each location and the multi-scale mean taken. Since this metric only accounts for recent mangrove loss, it likely underestimates long term loss of habitat. The mangrove estimated BHI score was calculated as the mean of the mangrove specific proportion and that of the extrapolated species level BHI (Figure 10). In parallel with the BHI, the first derivative of this proportion was taken.

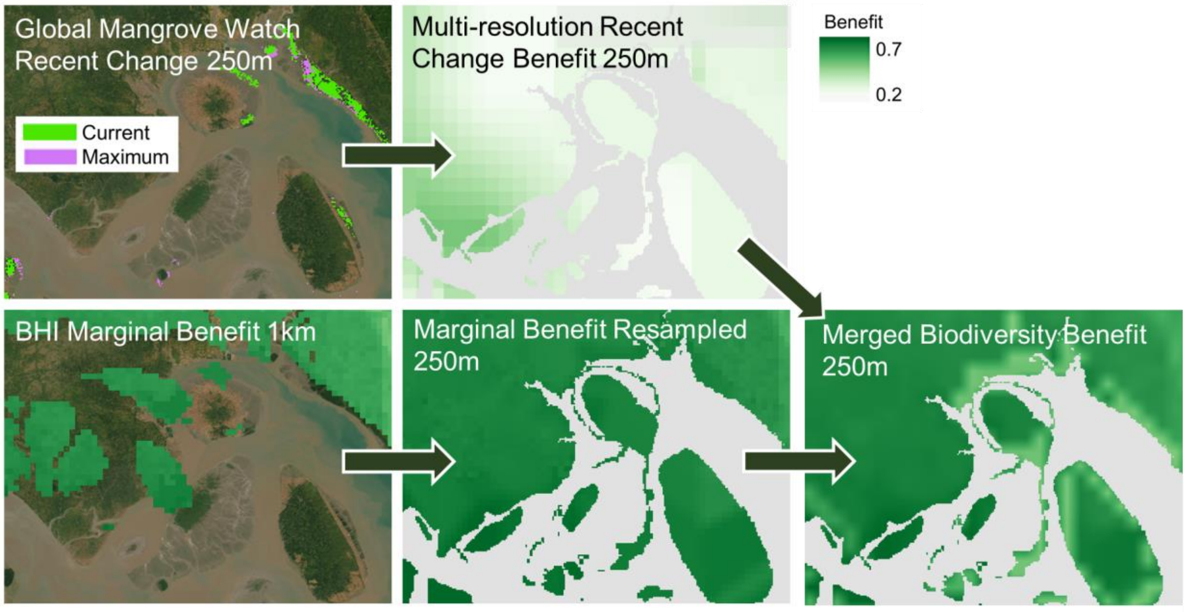

Figure 10 : Workflow for the calculation of a BHI index for mangroves (prior to calculating the first derivative for marginal benefit of restoration.

6.4 Carbon Benefits

6.4.1 Terrestrial systems

For terrestrial systems the additional carbon was calculated as the carbon content of forested areas in the geographical area. Soil carbon was excluded since the effects of tree restoration on soil carbon are complex and not yet fully understood. Potential tree carbon was estimated based on the above ground carbon density mapping of Spawn et al. (2020). The Copernicus Land Cover (Buchhorn et al., 2020) based tree mask (5.3.1) was used to mask out all non- tree areas. In order to extrapolate this observed forest cover to other nearby potential tree areas, the data was first smoothed using a low pass filter, and re-masked prior to applying a Euclidean allocation to fill the potential restoration mask, which was again smoothed using a low pass filter prior to superimposing the original data. The logic behind this is that the closest geographical native tree cover provides the best estimate of potential carbon for a new opportunity. Given wide variations in tree carbon as a function of local environment and species, this was considered a reasonable baseline approximation. This process is summarized in Figure 111 below.

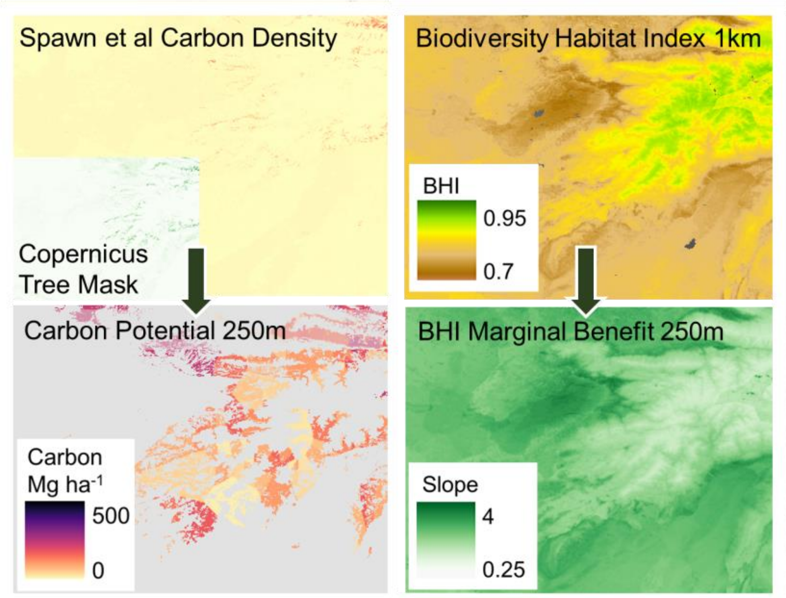

Figure 11: Calculation of carbon potential and biodiversity benefits for terrestrial systems

6.4.2 Mangrove systems

Mangrove additional carbon was calculated from first principles, following recent advances, but was broadly based on the NASA CMC (Simard, 2019) 30m above ground biomass data and the (Sanderman et al., 2018) 30m soil organic carbon (SOC) map. The approach used was the carbon accounting framework outlined in (Kauffman, 2012), which considers all aspects of the system rather than just these two datasets.

Whilst the Simard (2019) dataset represents living above ground biomass (ABG) it does not include either below ground biomass or dead wood. Below ground biomass (BGB) was derived from ABG, following the relationship in Komiyama et al. (2008) Fig. 4 (digitised using PlotDigitizer (2024)). This gives

$$BGB = e^{(0.9014 \ln AGB - 0.3662)}$$

ABG and BGB were converted into carbon (Mg ha^{-1}) using coefficients of 0.46 (ABG) and 0.39 (BGB) following Kauffman (2012) and Kauffman et al. (2020). Total mangrove plant structural carbon (MSC) can therefore be calculated directly as a function of AGB. Over the expected range of observed above ground biomass, (AGC+BGC) has a near linear response and can be approximated (R^2=0.99) as 0.62*AGB.

$$(AGC + BGC) = 0.48AGB + 0.39e^{(0.9014 \ln AGB - 0.3662)} \approx 0.62AGB$$

For dead wood, Mugi et al. (2022) show that quantities are highly, and this variation is likely dependent on socio-economic as well as ecological considerations. but have means of 16.85 Mg ha−1 (± 25.35) for standing dead and 29.92 Mg ha−1 (± 36.72) for downed wood which can be converted to carbon at the standard rates of 0.47 and 0.5 respectively (Kauffman, 2012) , giving a mean of 22.88 Mg ha-1 of dead wood.

Zhang et al. (2024) show that only 0.62 of SOC in marine mangrove ecosystems, and 0.49 in estuarine mangrove systems (as defined by (Spalding et al., 2016)) comes from mangroves, with the remainder coming from estuarine or marine sources. The Sanderman et al. (2018) SOC map covers only the top metre of the beach. To obtain the total carbon, this was combined with the SoildGrids 2017 data (Hengl et al., 2017) which was a source for the Sanderman layer was used for the 1 to 2m zone, extrapolating to mangrove beaches outside the SoilGrids mask using the 0-1m:1-2m SOC proportion as a baseline. After diving the mangrove opportunity areas into estuarine and coastal based on (Spalding et al., 2016), the two coefficients from Zhang et al. (2024) were applied to calculate the mangrove sourced carbon per grid cell.

This revised additional mangrove carbon approach (Figure 122) provides a more accurate but consistently lower carbon estimates than a simpler combination of the two remotely sensed datasets as in (Adame et al., 2021).

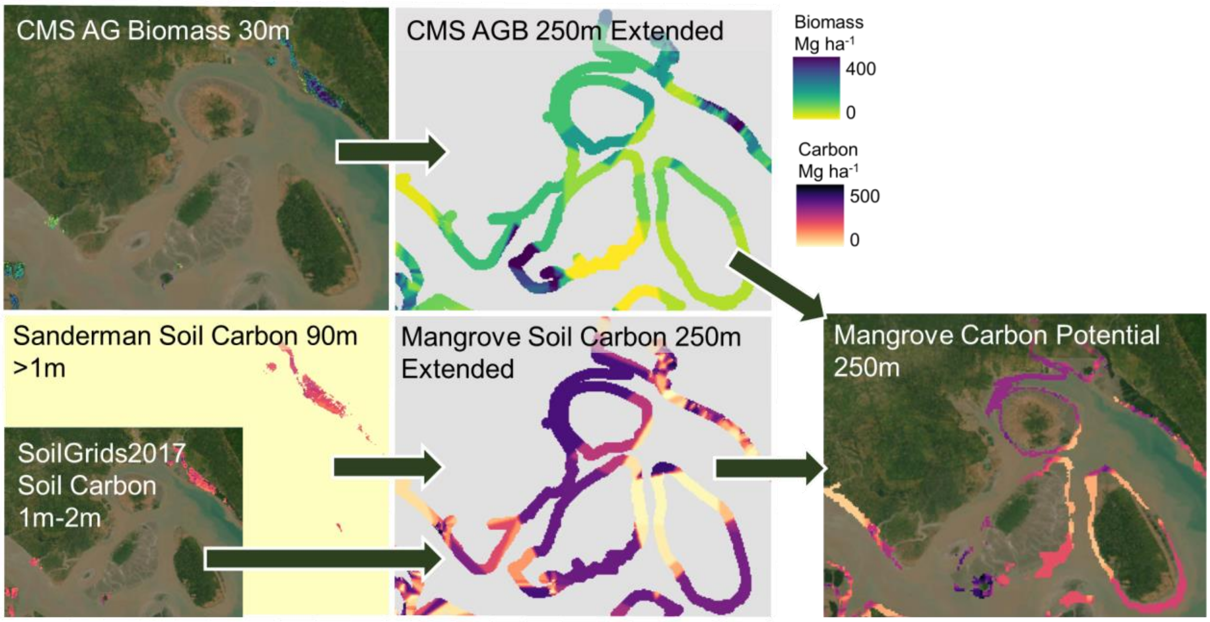

Figure 12 : Workflow for the calculation of additional mangrove carbon.

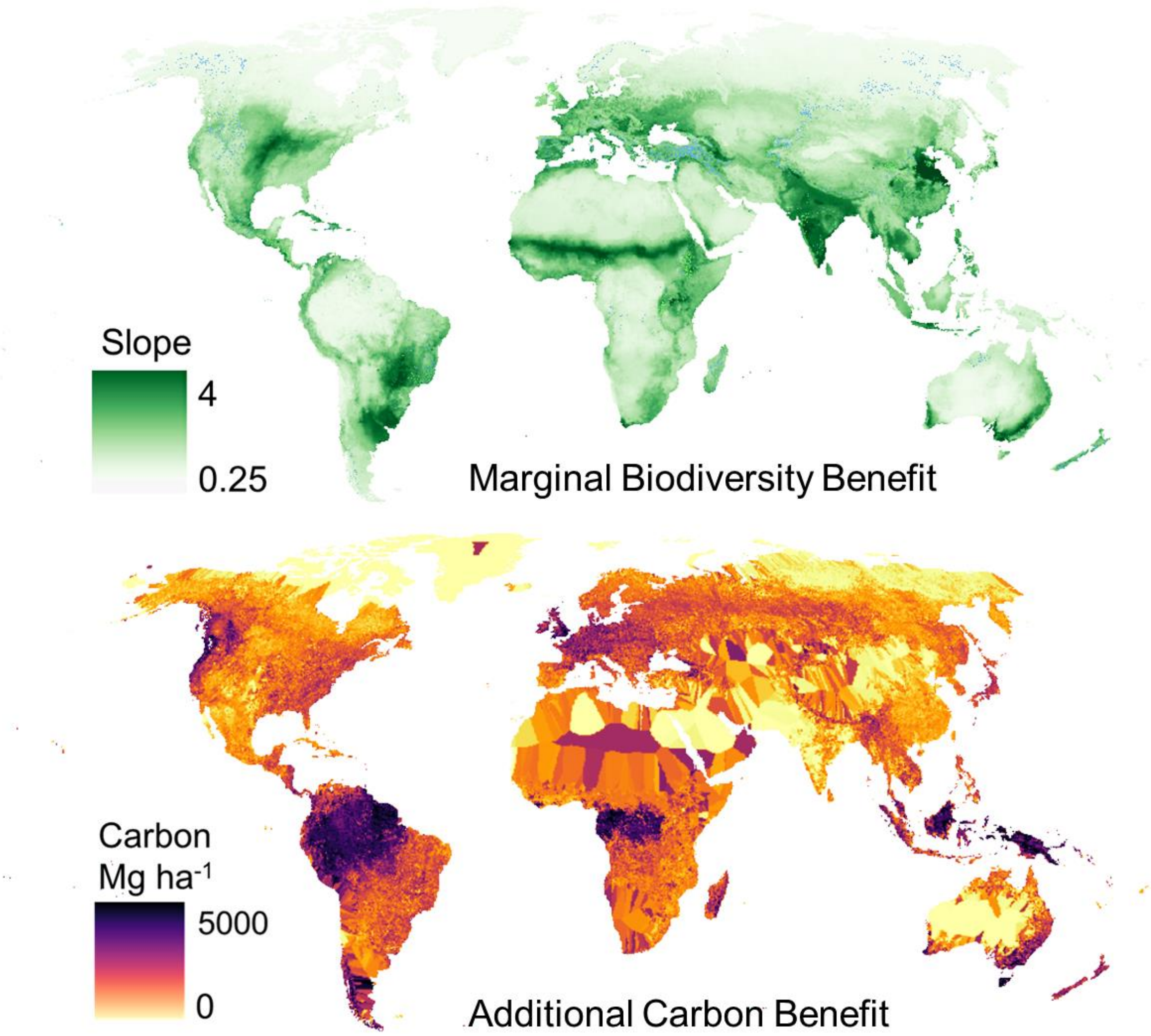

Figure 13 Global maps of tree carbon and biodiversity benefit. Note that these maps cover areas with no potential for tree cover, such as the Sahara Desert and Greenland where there is significant extrapolation,

6.4.3 Carbon Accumulation

The resultant carbon maps represent the expected carbon at maturity, at a nominal 50 years after planting. A simple carbon accumulation model was implemented to calculate the expected additional carbon at any time after either initiating natural regeneration or native planting, with a slight head start for carbon accumulation from native planting. This allows the wide variation in global accumulation rates to be represented by a single model based on carbon at maturity. Species and location specific modelling is recommended for final estimates. The typical sigmoid carbon accumulation curve was approximated using the flexible Richard's curve (Richards, 1959, Harwood and Hadley, 2009) or Generalised Logistic Curve, which allows parameterisation to meet a variable target height. Two curves were specified as a function of the target carbon at maturity *C*, and from which the lower limit *A* and upper limit *H* were calculated as *aC* and *hC* respectively.

$$Carbon_t = aC + \frac{hC}{\left(1 + Te^{[-B(t-M)]}\right)^{1/T}}$$

To be used, where the carbon at time *t* can be calculated as a function of the target carbon *C* using the parameters specified in Table 1 below for Natural regeneration and Native plantings respectively. Parameterisations were selected to achieve a slower initial accumulation rate for regeneration with the two curves converging at 30 years as the plot nears maturity. The resultant curves are plotted in for a target *C* value of 1000 Mg ha^{-1}

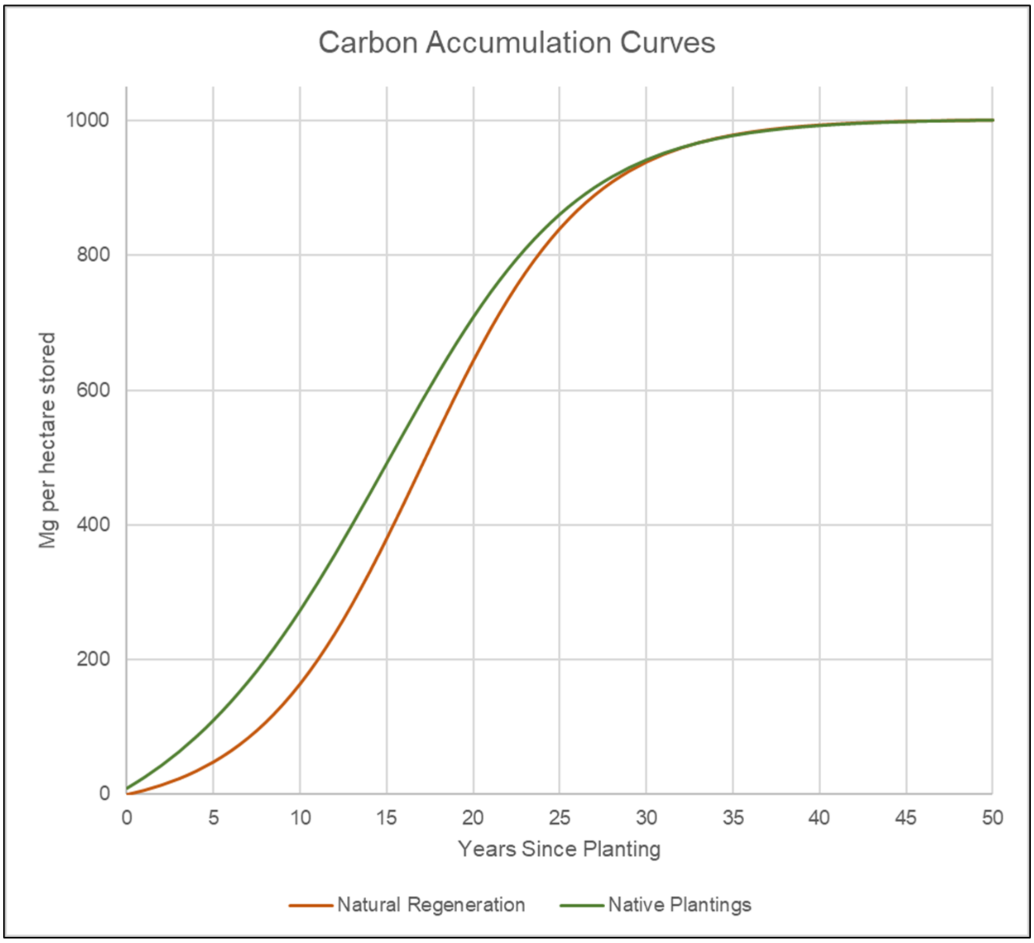

Figure 14 : Carbon accumulation curves to reach a target carbon at maturity of 1000 Mg ha^{-1}

Table 1: Parameters for carbon accumulation curves

Constant	*Natural regeneration*	*Native plantings*
h	***1.0295***	***1.117***
a	***0.0282***	***0.1152***
T	***1***	***1.5***
B	***0.21***	***0.19***
M	***17***	***15***

7. METHODS 3: RISKS, HAZARDS AND AVOIDED DAMAGES

7.1 Overview

Opportunity areas were derived from the raster suitability surfaces described in section 5.3, polygonised and split by level 12 HydroBasin catchments (Lehner, 2013). Each area was joined with attributes for planting and regeneration costs (USD/ha), biodiversity (relative index) and carbon benefits (t/ha), as described in section 6. Areas of potential slope vegetation for landslide risk reduction include a current land use attribute (bare, crops, or other) and areas of potential mangrove restoration include a shoreline attribute (accreting, slow-retreating or fast-retreating), as described in section 5.3.

Expected annual damages (EAD) or average annual losses (AAL), in terms of expected annual rehabilitation costs (USD) to road and rail assets from river and coastal flooding and landslides, were calculated based return period hazard maps and infrastructure assets within a buffer around each opportunity area. These data provide an upper bound on the potential avoided annual damages to infrastructure, without modelling the precise magnitude of the hazard reduction or risk reduction effect of any intervention.

The steps of the methodology described in this section are implemented in the open-source workflow, OpenGIRA (Open Global Infrastructure Risk/Resillience Analysis, Thomas et al. 2025). The resulting opportunity area data are available in the online GRI Risk Viewer[1] (Russell et al. 2025) for inspection and screening, filtered by administrative area and opportunity type, prioritised according to planting or regeneration cost, or infrastructure risk (EAD). They are also output in tabular format for ingestion into the Excel based opportunity investment tool (described in section 8 below) and in geospatial format for further spatial or quantitative analysis.

7.2 Hazards

Hazard data covers landslides, river and coastal flooding, represented as probability of occurrence (for landslides) or return period (RP) maps of hazard exceedance (for riverine and coastal flooding). Aqueduct river and coastal flooding and Deltares coastal flooding datasets including future epochs and climate scenarios, forced by downscaled global circulation model (GCM) outputs under one or more representative concentration pathways (RCPs). Other hazards include only the baseline present/historical case, as detailed in the table below.

Table 2: Hazard data sources with return periods and climate scenarios

Hazard	Dataset	Notes	Source
Landslide	World Bank	Hazard occurrence maps with annual probability of rainfall or earthquake triggered landslides.	ARUP (2021)
River flooding	Aqueduct	Flood inundation depth (m) return period maps, for multiple epochs, representative concentration pathways (RCPs), global circulation models (GCMs). **RP**: 2, 5, 10, 25, 50, 100, 250, 500, 1000 **Epoch**: baseline, 2030, 2050, 2080 **RCP**: baseline, 4.5, 8.5	Ward et al. (2020)

1 https://global.infrastructureresilience.org/

		GCM: GFDL-ESM2M, HadGEM2-ES, IPSL-CM5A-LR, MIROC-ESM-CHEM, NorESM1-M	
	JRC	Flood inundation depth (m) return period maps	Baugh et al. (2024)
		RP: 10, 20, 50, 75, 100, 200, 500	
Coastal flooding	Aqueduct	Flood inundation depth (m) return period maps, for multiple epochs and representative concentration pathways (RCPs).	Ward et al. (2020)
		RP: 2, 5, 10, 25, 50, 100, 250, 500, 1000	
		Epoch: baseline, 2030, 2050, 2080	
		RCP: baseline, 4.5, 8.5	
	Deltares	RP maps of flood inundation depth (m), for multiple epochs and digital elevation models (DEMs).	Deltares (2021)
		RP: 2, 5, 10, 25, 50, 100, 250	
		Epoch: baseline, 2050	
		RCP: baseline, 8.5	
		DEM: MERIT, NASA	

7.3 Infrastructure

Infrastructure assets for road and rail sectors were extracted from OpenStreetMap (2024). OpenStreetMap provides a consistent global, open dataset, with good coverage of major road and rail links. As a crowd-sourced dataset, quality and completeness are biased towards countries and regions with more active contributors, though the road network data has been assessed as highly complete and is actively maintained by a range of public and private actors (Barrington-Leigh and Millard-Ball 2017, Zhang et al. 2024).

Road assets were filtered on the "highway" tag to include roads classified from trunk down to tertiary in the source data. This classification system corresponds to mapping guidelines on the relative importance of roads within countries and may not relate directly to national road classes (OpenStreetMap 2025). Rail assets were filtered on the "railway" tag to include standard and narrow-gauge rail lines.

Table 3: Selected infrastructure sectors and asset types

Sector	Asset Types	Source
Road	Trunk, Motorway, Primary, Secondary, Tertiary	OpenStreetMap (2024)
Rail	Railway lines, standard or narrow gauge	

7.4 Risk

Risk to infrastructure was calculated in terms of direct damages, which estimate the cost required to make good any damage to physical assets, for example to clear and repair rail lines after inundation due to flooding, or to re-construct a road section after a destructive landslide.

In general, the process for estimating direct damages follows these steps:

- Intersect all assets with each hazard return period map
- Find the hazard intensity (e.g. flood depth) or probability of occurrence (of landslide) for each asset

- Identify a damage curve specific to the asset type and hazard combination
- Interpolate the hazard intensity value along the damage curve, calculating a damage fraction
- Multiply the damage fraction by the asset rehabilitation cost, giving a damage value for each return period
- Integrate under the loss-probability curve (defined by the set of return period damage values) to calculate expected annual damages

Linear elements (e.g. road or rail lines) are intersected with the regular grid defined by the hazard map and potentially split into many short segments, giving a hazard intensity and damage value for each line segment, which are summed to give asset-level risk estimates.

Rehabilitation cost assumptions were aggregated from multiple sources. Rail costs were taken from Koks et al (2019). Road costs were taken from Koks et al (2019) and US Federal Highways Agency (2020). Damage curves were taken from the recent review by Nirandjan (2024). Data tables are available within OpenGIRA[2] (Thomas 2025).

Every road and rail link was first intersected with each hazard map to give the hazard probability (for landslides, for each trigger) or hazard intensity (for river and coastal flooding, for each return period, model, return period, epoch, climate scenario, and other variants); then its damage fraction was calculated using piecewise linear interpolation of the damage curve; then damage value was calculated, either directly on an annual basis (for landslides, as only annual probability of landsliding was available), or for each return period; finally the expected annual damages were calculated, integrating numerically using Simpson's rule under the loss-probability curve defined by the set of return period damage values. Damages were summed back to the asset level, and summarised as minimum/mean/maximum values for each RCP and epoch, aggregating over GCMs in the case of Aqueduct river and coastal flooding, DEMs in the case of Deltares coastal flooding, and variations on the damage fraction in the case of landslides.

Limitations to this method include the lack of openly available data on asset vulnerability (damage and fragility curves), lack of detail on asset construction and condition, and broad global assumptions used for cost estimates.

7.5 Risk Reduction Benefits

Risks to infrastructure were linked with potential opportunity areas when they fell within a buffer of landslide-risk-reducing slope vegetation opportunities or coastal-flood-risk-reducing mangrove restoration opportunities, and within the same sub-basin river catchment (defined by level 12 HydroBasins, Lehner 2013) as river-flood-risk-reducing catchment restoration opportunities.

Table 4: Connection between opportunity areas and risks posed by related hazards

Opportunity	Hazard	Connected risks
Slope vegetation	Landslide	Assets at risk within 3km buffer of area
Mangrove restoration	Coastal flooding	Assets at risk within 5km buffer of area
Basin-scale restoration	River flooding	Assets at risk within the sub-basin

The opportunity areas were buffered and intersected with infrastructure assets, to find the set of assets within the potential area of effect of the intervention. The risks to that set of assets (expected annual direct damages posed by the relevant hazard) were summed to find the total EAD for the current or pre-intervention state. This is then taken as an upper bound on risk reduction, which allows directly to screen out potential opportunity areas with no nearby infrastructure at risk from relevant hazards and can be used to rank and prioritise opportunity areas according to maximum pre-intervention risk, both under present and future climate scenarios.

2 https://github.com/nismod/open-gira/tree/v0.3.2/config

8. METHODS 4: OPPORTUNITY INVESTMENT TOOL

8.1 Overview of the Dashboard

This section introduces a dashboard designed to support investment decision-making in Nature-based Solutions (NbS) by offering a structured, data-driven platform for project screening and prioritization. As NbS attract growing interest from investors—not only for their environmental value but also for their financial returns, carbon credit potential, and social co-benefits—the challenge lies in effectively identifying and comparing the most impactful investment opportunities. Balancing returns across financial, environmental, and social dimensions requires robust, transparent tools.

The dashboard addresses this need by enabling users to identify the best restoration areas based on financial feasibility and impact-driven metrics, and to compare different investment opportunities across hazards, restoration strategies, and projected benefits. It offers full customization for investors, allowing dynamic adjustment of metric weights to reflect their specific priorities—whether ROI, biodiversity, carbon sequestration, or social outcomes. By consolidating diverse metrics into a single platform and enabling systematic screening, analysis, and ranking of projects, the dashboard empowers investors to make more informed, targeted, and impactful decisions.

8.2 Total Opportunity Areas Considered

The dashboard compiles and evaluates a comprehensive global dataset of potential opportunity areas, each representing distinct geographic units suitable for implementing Nature-based Solutions (NbS). These areas are selected based on their ecological and biophysical characteristics, hazard exposure, restoration potential, and anticipated environmental. By systematically assessing these opportunity areas, the dashboard facilitates targeted investment and optimized intervention planning.

8.2.1 Hazards Targeted

The dashboard classifies NbS opportunities according to the climate-related hazards they aim to mitigate. The primary hazard categories include:

- Coastal Flooding: Coastal areas at risk from rising sea levels, storm surges, and coastal erosion.
- River Flooding: Inland regions prone to river overflow events, flash floods, or prolonged inundation.
- Landslides: Sloped areas susceptible to soil instability, erosion, and landslide events due to heavy rainfall or land degradation.

Each hazard type has unique risk profiles and corresponding restoration strategies, enabling investors to strategically prioritize interventions aligned with their resilience and mitigation goals.

8.2.2 Plantation Options

The dashboard differentiates NbS intervention strategies based on ecological suitability and hazard-specific requirements. Key plantation strategies include:

- Mangrove Restoration: Primarily for protecting and stabilizing coastal regions, reducing coastal flooding impacts, and enhancing biodiversity.
- Basin-Scale Tree Planting: Implemented at the watershed or basin level to enhance hydrological regulation, reduce river flood risks, and deliver catchment-wide ecological benefits.
- Slope Vegetation: Specifically suited to areas at risk of landslides, using targeted vegetation planting and slope stabilization techniques to reduce erosion and slope failure.

8.2.3 Restoration Classes

Within each restoration type, further classifications are used to reflect landscape conditions or trajectories, which influence restoration feasibility, cost, and expected outcomes:

- Mangrove Restoration Classes:
    - Accreting: Expanding coastlines that offer highly suitable conditions for successful mangrove restoration.
    - Slow Retreating: Coastlines experiencing gradual erosion or moderate retreat, suitable for managed restoration efforts.
    - Fast Retreating: Areas facing rapid erosion and severe habitat loss, where restoration is challenging and typically requires greater investment or innovative approaches.
- Landslide Restoration Classes:
    - Crops: Agricultural lands on slopes, requiring specific interventions to stabilize soils while balancing agricultural productivity.
    - Other: Mixed-use or degraded lands characterized by varying vegetation cover and erosion conditions, suitable for diverse restoration approaches.

These detailed classifications allow investors to precisely tailor NbS interventions to local ecological dynamics, enabling accurate assessments of potential impacts, feasibility, and effectiveness.

8.3 Key Metrics

The dashboard uses a suite of quantitative metrics to assess the performance and impact of Nature-based Solutions (NbS) projects across financial, environmental, and social dimensions. These indicators provide a standardized basis for comparing project options and informing investment decisions.

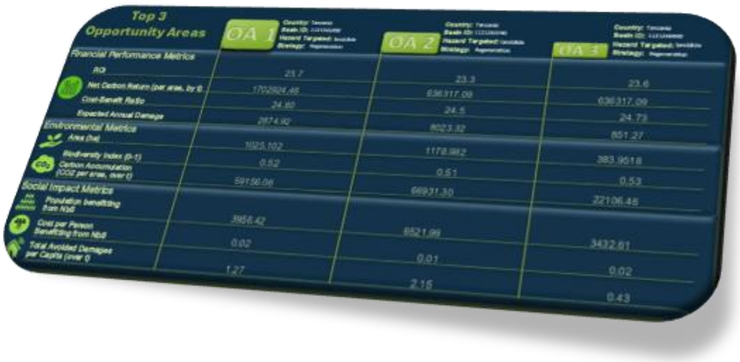

The dashboard draws upon multiple indicators, grouped under three main categories: Financial Metrics, Environmental Metrics, and Social Impact Metrics.

8.3.1 Financial Metrics

- ROI (Return on Investment): Measures the profit generated per dollar invested. A higher ROI indicates greater financial efficiency; values above 1 suggest a profitable project.
- Cost-Benefit Ratio (CBR): Reflects the financial viability of the project. A CBR greater than 1 means the project generates more value than it costs.
- Expected Annual Damage (EAD): Quantifies baseline economic losses to infrastructure from climate-related hazards, providing a proxy for risk exposure.

8.3.2 Environmental Metrics

- Biodiversity Index: Evaluates the marginal biodiversity benefit of restoration, based on spatially explicit data (e.g., 250-m resolution), capturing ecosystem integrity and habitat improvement.
- Carbon Accumulation: Measures total carbon sequestered by a project by year t, within a given area, indicating long-term climate mitigation potential.

8.3.3 Social Impact Metrics

- Population Benefiting from NbS: Refers to the population living adjacent to or within the hydrobasins targeted by the NbS intervention, who may directly benefit from reduced risk or enhanced ecosystem services.
- Avoided Damage per Capita: Assesses the extent to which individual exposure to damage is reduced, highlighting the equity and effectiveness of the intervention.
- Cost per Person Benefiting from NbS: Measures the social cost-efficiency of the intervention; lower values indicate a greater impact per dollar spent in terms of population reached.

8.3.4 Risk Reduction Metrics

Additionally, we further assess risk reduction metrics, estimating avoided damages as follows:

$$Avoided\ Damage\ per\ Capita = \frac{Risk\ Reduction\ Factor \cdot EAD}{Population\ Around\ the\ Hydrobasin}$$

- Avoided Damage per Capita: Measures how much risk reduction is provided to each individual within the affected population
- Estimated Avoided Damage: is equal to $Risk\ Reduction\ Factor \cdot EAD$, and measures the risk reduction applying a Risk Reduction Factor (RRF) based on the literature (see table 2).

Table 5: Risk Reduction Factors

Hazard	NbS Intervention	Class	Risk Reduction Factor (RRF)	Medium EAD Reduction (%)
Coastal Flooding	Mangroves	Accreting	40-60%	50
Coastal Flooding	Mangroves	Retreating	20-40%	30
Coastal Flooding	Mangroves	Retreating Fast	10-20%	15
River Flooding	Basin-Scale Tree Planting	N/A	10-30%	20
Landslides	Slope Vegetation	Other	30-70%	35
Landslides	Slope Vegetation	Bare	30-70%	35
Landslide	Slope Vegetation	Crops	10-30%	20

These metrics are integrated into a flexible scoring framework that allows investors to assign weights based on their priorities, supporting customized, multi-criteria decision-making.

8.4 1. Investor's Parameters and Scores

A set of parameters allows the end-user to customize input factors such as:

- Hazard(s) targeted (e.g., floods, droughts, etc.)
- Country-specific preferences
- Carbon price (USD/ton)
- Project timeframe (from 1 to 50 years)
- Reduction risk factor (e.g., low, medium, high)

8.4.1 Scores

The dashboard calculates both a Composite Score (integrating financial, risk reduction, and environmental performance) and a Social Impact Score, each built using customizable weightings. This structure supports comparison across NbS strategies and facilitates clear, evidence-based prioritization of investments.

The Composite Score is a weighted aggregate metric reflecting investor type or preference, encompassing:

- ROI (Return on Investment)
- Carbon Sequestration (or "Carbon Weight")
- Biodiversity Benefits (Biodiversity Index)
- Expected Annual Damage (EAD) Reduction

The Social Impact Score is a secondary aggregate metric emphasizing:

- Avoided Damage per Capita
- Carbon Benefit per Capita
- Population benefiting from NbS

8.4.2 Composite Score

To calculate the Composite Score, each primary indicator or metric is assigned a weight (w1, w2, w3, w4) according to the user's or investor's priorities.

Investor's parameters	Value
Hazard Targeted	All
Country	All
Carbon Price (USD/ton)	30
Project Timeframe (years)	7
Reduction Risk Factor	medium
Composite Score (reflecting investor's type)	
ROI Weight (w1)	0.5
Carbon Weight (w2)	0.1
Biodiversity Weight (w3)	0.1
EAD (w4)	0.2
Social Impact Score	
Avoided Damage per capita (w1)	0.25
Carbon Benefit per capita (w2)	0.25
Population (w3)	0.5

alues in red can be modified.
The sum of the weights must be uqual to 1.

- **ROI (Weight 1)**: Emphasizes economic returns.
- **Carbon Sequestration (Weight 2)**: Reflects importance of carbon sequestration and climate benefits.
- **Biodiversity (Weight 3)**: Reflects importance of ecological health and resilience.
- **EAD (Weight 4)**: Reflects importance of risk reduction (i.e., lowering expected annual damage).

The sum of these weights totals 1.0 in the Composite Score calculation, ensuring that changing one weight necessarily adjusts the others;

Once weights are chosen, the dashboard calculates a **Composite Score** as a weighted average:

$$\begin{aligned} Composite\ Score &= w1 \cdot (ROI\ Normalized) + w2 \cdot (Carbon\ Benefit\ Normalized) + w3 \\ &\cdot (Biodiversity\ Index\ Normalized) + w4 \cdot (EAD\ Reduction\ Normalized) \end{aligned}$$

N.B.: Each metric is typically normalized (e.g., min-max normalization) to ensure comparability on a 0–1 scale.

8.4.3 Social Impact Score

This is a parallel metric focusing on:

- **Population benefitting from NbS (Weight 1):** Emphasizes the population living next to the hydro basin affected by hazards.
- **Avoided Damage per Capita (Weight 2):** Reflects importance of the avoided impact per affected population.
- **Cost per person benefitting from NbS (Weight 3):** Reflects importance of social cost-efficiency.

$$\begin{aligned} Social\ Impact\ Score &= \alpha 1 \cdot (Avoided\ Damage\ per\ Capita) + \alpha 2 \cdot (Carbon\ Benefit\ per\ Capita) + \alpha 3 \\ &\cdot (Population\ Benefiting) \end{aligned}$$

Weights (α1,α2,α3) are adjustable based on user-preferences.

8.5 Top 10 Opportunity Areas Table

After calculating Composite Scores and Social Impact Scores, the tool presents a ranked list of the top 10 NbS opportunities. Each entry in the table represents an NbS project area, along with relevant country/region data, hazard targeted, and **displayed Indicators** may include:

- ROI
- Net Carbon Return
- Avoided Damage
- Cost-Benefit Ratio
- Cost per Person Benefiting

- o Social Impact Score

8.6 User Interaction and Prioritization Strategy

8.6.1 Investor Type Buttons

- ROI-Focused: Assigns heavier weight (e.g., 0.5) to ROI, with smaller allocations for carbon, biodiversity, and risk reduction.
- Carbon-Focused: Prioritizes carbon benefits with a higher weight for carbon sequestration.
- Biodiversity-Focused: Increases the biodiversity index weighting for ecologically minded investors.
- Balanced Approach: Spreads weights more evenly among ROI, carbon, biodiversity, and risk reduction.

Investor Type	ROI Weight (w1)	Carbon Weight (w2)	Biodiversity Weight (w3)	EAD (w4)	
ROI-Focused	0.5	0.1	0.1	0.2	1.Select
Carbon-Focused	0.2	0.5	0.1	0.2	1. Select
Biodiversity-Focused	0.2	0.2	0.4	0.2	1. Select
Balanced Approach	0.3	0.3	0.2	0.2	1. Select

N.B.: These parameters can be refined based on user-preferences.

8.6.2 Navigation Buttons

- Refresh: Recalculates the ranking or updates the table after any changes to carbon price, timeframe, or hazard preferences.
- Sort by Different Priorities: Quickly reorganizes the top 10 table by Composite Score or Social Impact Score.

8.7 Conclusion

The dashboard provides a powerful tool to support investment in Nature-based Solutions (NbS) by enabling optimized, transparent, and customizable decision-making. By integrating both financial and environmental metrics, it allows investors to systematically prioritize projects that offer the strongest combination of economic returns, climate risk reduction, and environmental or social impact. Its dynamic weighting system ensures flexibility, allowing users to tailor their focus—whether on ROI, biodiversity, carbon sequestration, or social benefits—according to their specific investment strategies. Ultimately, the dashboard underscores the dual value of NbS: their ability to mitigate climate hazards such as floods and landslides, while delivering tangible financial and societal gains. The top-ranked projects illustrate that nature-based investments can be both profitable and impactful, offering a data-driven path toward sustainable development and climate resilience.

9. ANNEXES

ANNEX 1. BIBLIOGRAPHY

ADAME, M. F., CONNOLLY, R. M., TURSCHWELL, M. P., LOVELOCK, C. E., FATOYINBO, T., LAGOMASINO, D., GOLDBERG, L. A., HOLDORF, J., FRIESS, D. A., SASMITO, S. D., SANDERMAN, J., SIEVERS, M., BUELOW, C., KAUFFMAN, J. B., BRYAN-BROWN, D. & BROWN, C. J. 2021. Future carbon emissions from global mangrove forest loss. *Global Change Biology,* 27**,** 2856-2866.

ALLNUTT, T. F., FERRIER, S., MANION, G., POWELL, G. V. N., RICKETTS, T. H., FISHER, B. L., HARPER, G. J., IRWIN, M. E., KREMEN, C., LABAT, J.-N., LEES, D. C., PEARCE, T. A. & RAKOTONDRAINIBE, F. 2008. A method for quantifying biodiversity loss and its application to a 50-year record of deforestation across Madagascar. *Conservation Letters,* 1**,** 173-181.

ARUP. 2021. Global Landslide Hazard Map, prepared for World Bank and Global Facility for Disaster Risk Reduction. [Dataset]. Available: https://datacatalog.worldbank.org/search/dataset/0037584

BARRINGTON-LEIGH, C. & MILLARD-BALL, A. 2017. The world's user-generated road map is more than 80% complete. PLoS ONE 12(8) e0180698.

BAUGH, C., COLONESE, J., D'ANGELO, C., DOTTORI, F., NEAL, J., PRUDHOMME, C. & SALAMON, P. 2024. Global river flood hazard maps. European Commission, Joint Research Centre (JRC) [Dataset] Available: data.europa.eu/89h/jrc-floods-floodmapgl_rp50y-tif

BAYRAKTAROV, E., SAUNDERS, M. I., ABDULLAH, S., MILLS, M., BEHER, J., POSSINGHAM, H. P., MUMBY, P. J. & LOVELOCK, C. E. 2016. The cost and feasibility of marine coastal restoration. *Ecological Applications,* 26**,** 1055-1074.

BRUN, P., ZIMMERMANN, N. E., HARI, C., PELLISSIER, L. & KARGER, D. N. 2022. Global climate-related predictors at kilometer resolution for the past and future. *Earth Syst. Sci. Data,* 14**,** 5573-5603.

BUCHHORN, M., LESIV, M., TSENDBAZAR, N.-E., HEROLD, M., BERTELS, L. & SMETS, B. 2020. Copernicus Global Land Cover Layers—Collection 2. *Remote Sensing,* 12**,** 1044.

BUNTING, P., ROSENQVIST, A., HILARIDES, L., LUCAS, R., THOMAS, N., TADONO, T., WORTHINGTON, T., SPALDING, M., MURRAY, N., & REBELO, L.-M. 2022. Global Mangrove Watch (1996 - 2020) Version 3.0 Dataset (3.0). Zenodo.

BUSCH, J., BUKOSKI, J. J., COOK-PATTON, S. C., GRISCOM, B., KACZAN, D., POTTS, M. D., YI, Y. & VINCENT, J. R. 2024. Cost-effectiveness of natural forest regeneration and plantations for climate mitigation. *Nature Climate Change,* 14**,** 996-1002.

DELTARES. 2021. Planetary computer and Deltares global data: Coastal flood hazard maps. [Dataset]. Available: https://ai4edatasetspublicassets.blob.core.windows.net/assets/aod_docs/11206409-003-ZWS-0003_v0.1-Planetary-Computer-Deltares-global-flood-docs.pdf

GEBCO_COMPILATION_GROUP 2023. GEBCO 2023 Grid. *In:* GROUP, G. C. (ed.).

GIJÓN MANCHEÑO, A., HERMAN, P. M. J., JONKMAN, S. N., KAZI, S., URRUTIA, I. & VAN LEDDEN, M. 2021. Mapping Mangrove Opportunities with Open Access Data: A Case Study for Bangladesh. *Sustainability* [Online], 13.

HARWOOD, T. D. & HADLEY, P. D. 2009. HDC Poinsettia Tracker: Flexible graphical tracking software. *Computers and Electronics in Agriculture,* 66**,** 215-217.

HARWOOD, T. W., C ; HOSKINS, A; FERRIER, S; BUSH, A ; GOLEBIEWSKI, M; HILL, S; OTA, N; PERRY,J; PURVIS, A; WILLIAMS, K . 2022. BHI v2: Biodiversity Habitat Index: 30s global time series. v1. *In:* CSIRO (ed.). CSIRO.

HAWKER, L. & NEAL, J. 2021. FABDEM V1-0.

HENGL, T. 2018. Global DEM derivatives at 250 m, 1 km and 2 km based on the MERIT DEM.

HENGL, T., MENDES DE JESUS, J., HEUVELINK, G. B. M., RUIPEREZ GONZALEZ, M., KILIBARDA, M., BLAGOTIĆ, A., SHANGGUAN, W., WRIGHT, M. N., GENG, X., BAUER-MARSCHALLINGER, B., GUEVARA, M. A., VARGAS, R., MACMILLAN, R. A., BATJES, N. H., LEENAARS, J. G. B., RIBEIRO, E., WHEELER, I., MANTEL, S. & KEMPEN, B. 2017. SoilGrids250m: Global gridded soil information based on machine learning. *PLOS ONE,* 12, e0169748.

HENGL, T., WALSH, M. G., SANDERMAN, J., WHEELER, I., HARRISON, S. P. & PRENTICE, I. C. 2018. Global mapping of potential natural vegetation: an assessment of machine learning algorithms for estimating land potential. *PeerJ,* 6, e5457.

HOSKINS, A. J., HARWOOD, T. D., WARE, C., WILLIAMS, K. J., PERRY, J. J., OTA, N., CROFT, J. R., YEATES, D. K., JETZ, W., GOLEBIEWSKI, M., PURVIS, A., ROBERTSON, T. & FERRIER, S. 2020. BILBI: Supporting global biodiversity assessment through high-resolution macroecological modelling. *Environmental Modelling & Software,* 132, 104806.

HUDSON, T., KEATING, K. & PETTIT, A. 2015. Cost estimation for coastal protection –summary of evidence. Bristol: Environment Agency.

KASAI, M. & YAMADA, T. 2019. Topographic effects on frequency-size distribution of landslides triggered by the Hokkaido Eastern Iburi Earthquake in 2018. *Earth, Planets and Space,* 71, 89.

KAUFFMAN, J. B., ADAME, M. F., ARIFANTI, V. B., SCHILE-BEERS, L. M., BERNARDINO, A. F., BHOMIA, R. K., DONATO, D. C., FELLER, I. C., FERREIRA, T. O., JESUS GARCIA, M. D. C., MACKENZIE, R. A., MEGONIGAL, J. P., MURDIYARSO, D., SIMPSON, L. & HERNÁNDEZ TREJO, H. 2020. Total ecosystem carbon stocks of mangroves across broad global environmental and physical gradients. *Ecological Monographs,* 90, e01405.

KAUFFMAN, J. B. D., D. 2012. Protocols for the measurement, monitoring and reporting of structure, biomass and carbon stocks in mangrove forests. Bogor: CIFOR.

KOKS, E.E., ROZENBERG, J., ZORN, C. et al. A global multi-hazard risk analysis of road and railway infrastructure assets. *Nature Communications* 10, 2677 (2019).

KOMIYAMA, A., ONG, J. E. & POUNGPARN, S. 2008. Allometry, biomass, and productivity of mangrove forests: A review. *Aquatic Botany,* 89, 128-137.

KULP, S. & STRAUSS, B. H. 2024. CoastalDEM v3.0: Improving fully global coastal elevation predictions through a convolutional neural network and multi-source DEM fusion. .

LAN, H., WANG, D., HE, S., FANG, Y., CHEN, W., ZHAO, P. & QI, Y. 2020. Experimental study on the effects of tree planting on slope stability. *Landslides,* 17, 1021-1035.

LEHNER, B., GRILL G. 2013. Global river hydrography and network routing: baseline data and new approaches to study the world's large river systems. *Hydrological Processes,* 27, 2171–2186.

LI, Y. & DUAN, W. 2024. Decoding vegetation's role in landslide susceptibility mapping: An integrated review of techniques and future directions. *Biogeotechnics,* 2, 100056.

LUIJENDIJK, A., HAGENAARS, G., RANASINGHE, R., BAART, F., DONCHYTS, G. & AARNINKHOF, S. 2018. The State of the World's Beaches. *Scientific Reports,* 8, 6641.

LYARD, F. H., ALLAIN, D. J., CANCET, M., CARRÈRE, L. & PICOT, N. 2021. FES2014 global ocean tide atlas: design and performance. *Ocean Sci.,* 17, 615-649.

MCCOLL, S. T. & COOK, S. J. 2024. A universal size classification system for landslides. *Landslides,* 21, 111-120.

MUGI, L. M., KISS, D., KAIRO, J. G. & HUXHAM, M. R. 2022. Stocks and Productivity of Dead Wood in Mangrove Forests: A Systematic Literature Review. *Frontiers in Forests and Global Change,* 5.

OPENSTREETMAP. 2024. *OpenStreetMap Planet File*. [Online]. Available: https://www.openstreetmap.org [Accessed 4 November 2024].

OPENSTREETMAP. 2025. Highways. *OpenStreetMap Wiki.* [Online]. Available: https://wiki.openstreetmap.org/wiki/Highways#Classification [Accessed 28 March 2025].

PAULSEN, J. & KÖRNER, C. 2014. A climate-based model to predict potential treeline position around the globe. *Alpine Botany,* 124, 1-12.

PLOTDIGITIZER. 2024. *PlotDigitizer, 3.1.6* [Online]. Available: https://plotdigitizer.com [Accessed].

REDSHAW, P., BOTTOMLEY, J 2020. The Global Landslide Hazard Map: Final Project Report. The World Bank.

RICHARDS, F. J. 1959. A Flexible Growth Function for Empirical Use. *Journal of Experimental Botany,* 10, 290-300.

RUSSELL, T., ZIARKOWSKI, M., THOMAS, F., NICHOLAS, C., PANT, R., BERNHOFEN, M., JARAMILLO, D., LEONOVA, N., SHIARELLA, A., LESTANG, T., ROBERTSON, M., LEMMEN, R., GLASGOW, G., FOWLER, T., RANGER, N. & HALL, J.W. 2025. GRI (Global Resilience Index) Risk Viewer. [Online] https://global.infrastructureresilience.org/ [Accessed 28 March 2025].

SANDERMAN, J., HENGL, T., FISKE, G., SOLVIK, K., ADAME, M. F., BENSON, L., BUKOSKI, J. J., CARNELL, P., CIFUENTES-JARA, M., DONATO, D., DUNCAN, C., EID, E. M., ERMGASSEN, P. Z., LEWIS, C. J. E., MACREADIE, P. I., GLASS, L., GRESS, S., JARDINE, S. L., JONES, T. G., NSOMBO, E. N., RAHMAN, M. M., SANDERS, C. J., SPALDING, M. & LANDIS, E. 2018. A global map of mangrove forest soil carbon at 30 m spatial resolution. *Environmental Research Letters,* 13, 055002.

SAYRE, R., NOBLE, S., HAMANN, S., SMITH, R., WRIGHT, D., BREYER, S., BUTLER, K., VAN GRAAFEILAND, K., FRYE, C., KARAGULLE, D., HOPKINS, D., STEPHENS, D., KELLY, K., BASHER, Z., BURTON, D., CRESS, J., ATKINS, K., VAN SISTINE, D. P., FRIESEN, B., ALLEE, R., ALLEN, T., ANIELLO, P., ASAAD, I., COSTELLO, M. J., GOODIN, K., HARRIS, P., KAVANAUGH, M., LILLIS, H., MANCA, E., MULLER-KARGER, F., NYBERG, B., PARSONS, R., SAARINEN, J., STEINER, J. & REED, A. 2019. A new 30 meter resolution global shoreline vector and associated global islands database for the development of standardized ecological coastal units. *Journal of Operational Oceanography,* 12, S47-S56.

SIMARD, M., T. FATOYINBO, C. SMETANKA, V.H. RIVERA-MONROY, E. CASTANEDA, N. THOMAS, AND T. VAN DER STOCKEN. 2019. Global Mangrove Distribution, Aboveground Biomass, and Canopy Height. *In:* ORNL DAAC, O. R., TENNESSEE, USA. (ed.). ORNL DAAC, Oak Ridge, Tennessee, USA.

SPALDING, M., BRUMBAUGH R.D. & E., L. 2016. Atlas of Ocean Wealth. Arlington, VA: The Nature Conservancy.

SPAWN, S. A., SULLIVAN, C. C., LARK, T. J. & GIBBS, H. K. 2020. Harmonized global maps of above and belowground biomass carbon density in the year 2010. *Scientific Data,* 7, 112.

THOMAS, F., RUSSELL, T., LESTANG, T., ROBERTSON, M. & FERNANDEZ-PEREZ, A. 2025. OpenGIRA, nismod/open-gira: v0.3.2. Zenodo. https://doi.org/10.5281/zenodo.15011305

UNCBD 2022. Decision Adopted by the Conference of Parties to the Convention on Biological Diversity 15/4. Kunming-Montreal Global Biodiversity Framework. UN Convention On Biological Diversity.

US FEDERAL HIGHWAYS AGENCY. 2020. Bridge Replacement Unit Costs 2020. Available: https://www.fhwa.dot.gov/bridge/nbi/sd2020.cfm

VAN GRAAFEILAND, K. 2020. Global Tidal Range Classification.

WARD, P.J., H.C. WINSEMIUS, S. KUZMA, M.F.P. BIERKENS, A. BOUWMAN, H. DE MOEL, A. DÍAZ LOAIZA, et al. 2020. Aqueduct Floods Methodology. Technical Note. Washington, D.C.: World Resources Institute. Available: www.wri.org/publication/aqueduct-floods-methodology

WORLD BANK. 2008. Road Costs Knowledge System (ROCKS) v2.3. [Dataset]. Available: https://datacatalog.worldbank.org/search/dataset/0065670/Road-Costs-Knowledge-System--ROCKS

WORLD BANK. 2022. The Economics of Large-scaleMangrove Conservation and Restoration in Indonesia: Breifing Note. Technical Summary. The World Bank.

ZHANG, J., GAN, S., YANG, P., ZHOU, J., HUANG, X., CHEN, H., HE, H., SAINTILAN, N., SANDERS, C. J. & WANG, F. 2024. A global assessment of mangrove soil organic carbon sources and implications for blue carbon credit. *Nature Communications,* 15, 8994.

ZHANG, X., AN, J., ZHOU, Y., YANG, M. & ZHAO, X. 2024. How sustainable is OpenStreetMap? Tracking individual trajectories of editing behavior. *International Journal of Digital Earth,* 17(1).

Environmental Change Institute
University Centre for the Environment
University of Oxford
South Parks Road
Oxford OX1 3QY, UK
www.eci.ox.ac.uk

GLOBAL
CENTER ON
ADAPTATION

ANTOINE PLATEKADE 1006
3072 ME ROTTERDAM
THE NETHERLANDS
+31(0)88-088-6800
WWW.GCA.ORG